Journal of Materials Chemistry B

ROYAL SOCIETY OF CHEMISTRY

PAPER

View Article Online
View Journal | View Issue

Check for updates

Cite this: J. Mater. Chem. B, 2024, 12, 5711

Long-term antifouling surfaces for urinary catheters†

Mustafa Tüfekçi,[a] Sena Hamarat,[a] Tuğba Demir Çalışkan,[b] Hatice Ferda Özgüzar,[cd] Ahmet Ersin Meydan,[e] Julide Sedef Göçmen,[f] Ebru Evren,[g] Mehmet İlker Gökçe[h] and Hilal Goktas *[a]

The presence of a variety of bacteria is an inevitable/indispensable part of human life. In particular, for patients, the existence and spreading of bacteria lead to prolonged treatment period with many more complications. The widespread use of urinary catheters is one of the main causes for the prevalence of infections. The necessity of long-term use of indwelling catheters is unavoidable in terms of the development of bacteriuria and blockage. As is known, since a permanent solution to this problem has not yet been found, research and development activities continue actively. Herein, polyethylene glycol (PEG)-like thin films were synthesized by a custom designed plasma enhanced chemical vapor deposition (PE-CVD) method and the long-term effect of antifouling properties of PEG-like coated catheters was investigated against *Escherichia coli* and *Proteus mirabilis*. The contact angle measurements have revealed the increase of wettability with the increase of plasma exposure time. The antifouling activity of surface-coated catheters was analyzed against the Gram-negative/positive bacteria over a long-term period (up to 30 days). The results revealed that PE-CVD coated PEG-like thin films are highly capable of eliminating bacterial attachment on surfaces with relatively reduced protein attachment without having any toxic effect. Previous statements were supported with SEM, XPS, FTIR spectroscopy, and contact angle analysis.

Received 15th February 2024,
Accepted 1st May 2024

DOI: 10.1039/d4tb00311j

rsc.li/materials-b

Open Access Article. Published on 07 May 2024. Downloaded on 12/5/2025 8:51:53 PM.
This article is licensed under a Creative Commons Attribution-NonCommercial 3.0 Unported Licence.

1. Introduction

Infections that develop in parallel with the widespread use of implantable medical devices, which are frequently used in healthcare in the diagnosis and treatment of diseases, are an important cause of mortality and morbidity rates.[1] More than 65% of healthcare-associated infections (HAIs) are associated with implants or medical devices.[2] In particular, catheter-associated urinary tract infections (CAUTIs) are one of the most common causes of infection[3] and show systemic spread with a high (32.8%) mortality rate.[4] The main cause of catheter-related infection is prolonged presence in the urinary tract, resulting from catheterization of the bladder for 48 hours or longer.[5] The period of prolonged presence provides bacteria with an opportunity to adhere to catheter surfaces, allowing them to produce biofilms and develop antibiotic resistance.[6] Urinary catheter surfaces have certain properties that promote or attract microorganisms on the surfaces;[7] for example, non-uniform surface production during manufacturing[8] paves the way for a thin protein coating accumulated on the outer surface, which is very attractive for binding and growth.[9] While urine runs down, the mineral content leaves a trace for bacterial attachment and biofilm formation that leads to encrustation of the catheter. Regarding patients' health, in clinics, there is a growing need for outer and inner protective layers on catheters for the inhibition of bacterial attachment.

Numerous methods have been studied and practiced for the development of such a protective coverage; yet, majority of them still do not have adequate effectiveness. In terms of methods, there are two main ways to inhibit bacterial attachment, either by the use of antibiotics/antimicrobials or through antifouling coatings. The prominent characteristic of antifouling coatings is that they do not induce resistance in bacteria;[10]

[a] Department of Biomedical Engineering, Ankara University, Golbasi, Turkey. E-mail: hgoktas@ankara.edu.tr
[b] Department of Chemical Engineering, Ankara University, Turkey
[c] Plasma Aided Biomedical Research Group (pabmed) Biomedical Engineering Division, Graduate School of Engineering and Science, TOBB university of Economics and Technology, Ankara, 06560, Turkey
[d] Department of Materials Engineering, Biomaterials and Tissue Engineering Research Group, KU Leuven, Leuven, 3000, Belgium
[e] Department of Molecular Medicine, Graduate School of Health Sciences, TOBB University of Economics and Technology, Ankara, 06560, Turkey
[f] Department of Medical Microbiology, Faculty of Medicine, TOBB University of Economics and Technology, Ankara, 06560, Turkey
[g] Department of Medical Microbiology, Ankara University School of Medicine, Turkey
[h] Department of Urology, Ankara University School of Medicine, Turkey

† Electronic supplementary information (ESI) available. See DOI: https://doi.org/10.1039/d4tb00311j

Open Access Article. Published on 07 May 2024. Downloaded on 12/5/2025 8:51:53 PM.
This article is licensed under a Creative Commons Attribution-NonCommercial 3.0 Unported Licence.

therefore, unlike antibiotics, repeated exposure to antifouling coatings does not cause any adaptation. Polyethylene glycol (PEG) and its derivatives[10] and zwitterionic polymers are widely used as antifouling coatings in biomedical applications.[11,12] In general, surface modification of catheters with hydrophilic polymers can be carried out *via* physical adsorption or chemical binding of polymer chains. Compared to physical adsorption, chemical binding is more robust and long-lasting.[13] Solution processes and/or vacuum-assisted processes can be employed to produce chemically functionalized thin films on biomaterials. Solution processes are also known as wet thin film coating techniques which include dip coating, spin coating, spray coating, blade coating, and roll coating;[14] each has its own advantages, such as ease of coating and low-cost, with drawbacks of excessive use of monomer coating, *etc.* On the other hand, vacuum-assisted processes such as plasma-enhanced chemical vapor deposition (PE-CVD) are also being developed as an alternative method to overcome disadvantages of the solution process.[15] PE-CVD is the one of the crucial methods for solvent-free synthesis of polymer thin films in a single step. Since PE-CVD does not require any organic solvents and initiators, it avoids any coating defects such as dewetting from the substrates[16] and formation of aggregates.[17] Additionally, the ''low pressure'' environment of the method provides protection over sample surfaces and integrity of coatings.[18] This low-pressure environment makes monomer precursors to evaporate at lower temperatures rather than their boiling point. Therefore, easier and more controlled film thicknesses are achieved.[19,20] Addition of plasma intervention to the system even reduces the required temperature for deposition.[19]

It is well known that polyethylene glycol (PEG) polymers, also referred to as polyethylene oxide (PEO), have attracted considerable interest in the biomedical field for drug delivery,[21] tissue engineering[22] and surface modification of medical devices and implants due to their non-toxicity, good biocompatibility and biodegradability, non-immunogenicity, protein adhesion inhibition and antifouling properties.[23] PEG consists of $-CH_2CH_2O-$ repeating units and a hydroxy (–OH) group at the end of the polymer chain and the molecular weights of ethylene groups vary from 200 to 7 000 000 g mol^{-1} and those with lower molecular weights are referred to as polyethylene glycol, whereas ones with higher molecular weights are referred to as polyethylene oxide.[24] Over the decades, numerous studies have focused on the fabrication of effective PEG-like coatings to prevent bacterial adhesion and protein adsorption.[25] Although different approaches have been applied for PEG modification, plasma polymerization is the mainstay approach to obtain antifouling thin films (in nanoscale) and uniform PEG-like films.[26] The surface density of the CH_2CH_2O moieties known as ''PEO character'' is the most important parameter since the antifouling properties of PEO-like films depend on the PEO character. In other words, fouling behavior on surfaces can be adjusted by changing the PEO character.[27,28] López *et al.* were the first to prepare antifouling coatings by glow discharge at low pressures in vapors of tetraethylene glycol dimethyl ether (tetraglyme). They found that the films had high short-term resistance to protein adsorption (fibrinogen, albumin, and immunoglobulin G (IgG)) and cell adhesion (endothelial cell).[29] Then, numerous researchers have worked on the synthesis of PEO-like coatings through plasma-polymerization methods using various plasma precursors to create antifouling thin film coatings. Various ether-bearing precursors have been explored for this purpose. For instance, ethylene glycol dimethyl ether[30] and tetraglyme[31] stand out as some of the most commonly used precursors in plasma-polymerization processes.

PEG polymers with different molecular weights are also used as precursors for plasma-polymerization. As a plasma precursor monomer, PEG200 was only studied by Choi *et al.* to obtain PEG-like coatings *via* the capacitively coupled plasma chemical vapor deposition (CCP-CVD) method by applying a 2 W RF power for 30 min. It is reported that the PEG-like thin film is a biocompatible material and exhibits a high fibroblast cell repellency with low serum adsorption.[32] Amine-functionalized PEG-like thin films were prepared through the PE-CVD process, in which the plasma power varied from 2 W to 20 W (specifically, at 2, 5, 7, 10, and 20 W), to prevent non-specific protein adsorption (NSA).[26] The study by Kim *et al.* demonstrated that maximum inhibition of NSA was achieved when utilizing a plasma power of 5 W.[26] However, there are no reports on bacterial activity of PEG200 plasma-polymerized thin films.

When analyzing the basis of CAUTIs, two types of bacteria play a major role in the development of infections, which are *Escherichia coli* and *Proteus mirabilis.*[33] In particular, *E. coli* corresponds to 80% of the UTI[34] and 24% of the CAUTI cases, and it's quite renowned for its antibiotic resistance, which makes it difficult to eliminate from the urinary tract.[35] Similarly, *P. mirabilis* has a high infection rate[36] and is the main cause of crystal biofilm formation through the production of the urease enzyme. The interaction of this enzyme with urea causes the formation of struvite stones, which is one of the most known reasons for catheter obstruction.[37]

In the literature, the effectiveness of PEG-like coatings against undesired bacterial attachment and biofilm formation has been investigated for only up to a few days.[38] However, for CAUTIs, long-term studies are required to inhibit bacterial attachment and encrustation formation. In accordance with the need for further investigation, our group developed PEG-like thin films to provide a new potential catheter substrate for clinic applications that is capable of inhibiting long-term bacterial attachment with proven biocompatibility and non-toxicity.

In this work, PEG-like thin films were deposited on different substrates using the PE-CVD process at 5.0 W with different plasma exposure times. PEG200 was used as a plasma precursor due to its low molecular weight, which provides a lower evaporation point. And due to the low-pressure environment of the reactor, it evaporates even at lower temperatures (lower than the evaporation point), which helps maintain the chemical structure and proper bonding of monomer molecules. The antifouling behavior of the synthesized thin films was investigated by controlling the attachment of *P. mirabilis* and *E. coli* to the surfaces. Besides structural analysis, the interactive

 This journal is © The Royal Society of Chemistry 2024

Open Access Article. Published on 07 May 2024. Downloaded on 12/5/2025 8:51:53 PM. This article is licensed under a Creative Commons Attribution-NonCommercial 3.0 Unported Licence.

activity of PEG-like surfaces, protein adhesion, and *in vitro* cell viability were also examined.

2. Materials and methods

2.1 Substrates and chemicals

PEG-like films were synthesized using the PEG200 precursor as purchased from Sigma Aldrich. Urinary catheters were purchased from Rusch Foley Catheter 14Fr. Glass slides and Si wafers were cut into the size of 1.0 cm × 1.0 cm and catheters were cut into 1.0 cm-long segments. Dulbecco's minimum essential medium (DMEM), fetal bovine serum (FBS), Dulbecco's phosphate buffered saline (DPBS), and 3-(4,5-dimethylthiazol-2-yl)-2,5-diphenyltetrazolium bromide (MTT) were purchased from Sigma-Aldrich. L-Glutamine, penicillin–streptomycin, and 0.25% trypsin–0.005% EDTA were acquired from Biological Industries Ltd. NCTC clone 929 (L cell, L-929, derivative of Strain L; CCL-1™) mouse fibroblast cell line was supplied by American Type Culture Collection (ATCC). Tryptic soy agar (TSA), tryptic soy broth (TSB), dimethyl sulfoxide (DMSO) and ethanol were purchased from Merck Millipore.

2.2. Preparation of PEG-like films and their characterization

PEG-like films were synthesized by the following procedure. The PE-CVD system used in the process is illustrated in Fig. S1 (ESI†), and detailed information about all parts of the system can be found in the ESI† (S1). First, substrates were carefully positioned inside the deposition chamber. They were placed above the plasma shower ring head, which was directly connected to the chamber. Prior to the deposition, all substrates were washed with ethanol and deionized water, each repeated three times. Subsequently, they were dried using N_2. During film formation, the PEG precursor was vaporized at 140 °C within a glass tube connected to the plasma deposition chamber through the stainless distribution line. The PEG vapor pressure was set to 20 mTorr by adjusting the volumetric flow rate of precursor vapor. PEG polymerization was carried out at 5 W RF power for varying durations of 15, 30 and 60 min. Subsequently, all coated samples were kept under vacuum conditions at room temperature before undergoing characterization and microbiological studies. PEG-like films were labelled based on their exposure time, denoted as P15, P30 and P60. The chemical structure of PEG-like films was analyzed using attenuated total reflectance Fourier transform infrared spectroscopy (ATR-FTIR). The spectra of the films were acquired using a JASCO FTIR 4600 FTIR spectrometer. The surface chemical composition of the PEG-like film was further examined using X-ray photoelectron spectroscopy (XPS) with a PHI 5000 VersaProbe spectrometer. To assess the wettability of films, contact angle measurements were performed with deionized water and diiodomethane at room temperature using the sessile drop method. Results were recorded on a drop shape analysis instrument (KSV Instruments Ltd, Finland). The plasma polymerization technique is almost substrate independent and, especially in our case, since all three substrates are non-conductive materials, they will not be able to interfere with the RF plasma. Hence, FTIR analysis was carried out on coated silicone wafers, and XPS and contact angle analyzes were performed on glass slides. The antifouling, protein adhesion and cell viability analyses were conducted on Rusch Foley Catheter 14Fr silicone catheters.

2.3. *In vitro* antimicrobial/antifouling testing

A series of experiments were conducted to determine the antifouling features of the P60-coated urinary catheters (UCs) and uncoated UCs against two Gram-negative bacterial strains: *Proteus mirabilis* (ATCC 15146) and *Escherichia coli* (ATCC 25922) using procedure described elsewhere.[39] Specifically, *P. mirabilis* and *E. coli* strains were incubated in a tryptic soy broth (TSB) medium, and 10 μl of bacteria cells (1.5×10^6 CFU ml^{-1}) were inoculated on both uncoated UC and P60-coated UC surfaces and then they were covered with an acetate film to limit evaporation of the medium. All samples were incubated with each bacterial strain for 1, 3, 7 and 30 days at 37 °C (~15% humidity). At the end of each incubation duration, samples were detached from the acetate coverage, placed in a fresh UV-sterilized PBS (pH: 7.4), and gently washed to remove unbound bacteria. The concentration of live bacteria in the washing solution was analyzed after culturing in tryptic soy agar (TSA) plates. In addition to this analysis, the rinsed samples were also transferred to the centrifuge tubes containing 1 ml of fresh TSB medium and vortexed for 1 min to detach all the remaining bacteria on the catheter surface of the samples (uncoated UCs and P60-coated UCs). The remaining TSB suspensions consisting of bacteria were diluted ($1/10^3$, $1/10^5$ and, $1/10^7$) by fresh TSB addition and then cultured at 37 °C for 24 hours in TSA plates. This approach enables us to examine the surface behavior of films, which can either kill the bacteria upon contact or repel them from diffusing through the material surface. Ultimately, bacterial viability was analyzed by counting the number of colonies formed on the agar plates. The calculation formula used is as follows:

$$\text{Inhibition}\,(\%) = \frac{\#\text{ of bacteria on uncoated UCs} - \#\text{ of bacteria on coated UCs}}{\#\text{ of bacteria on uncotaed UCs}} \times 100$$

2.4. Protein adhesion studies

To investigate protein features of P60-coated urinary catheters (UCs), bovine serum albumin (BSA, Sigma Aldrich, ≥%96) was used as a model protein. Specifically, P60-coated and uncoated UCs were treated with BSA solution at a concentration of 1 mg ml^{-1} (in PBS, 0.1 M, pH: 7.4). The samples were placed in BSA in a shaker incubator at 50 rpm at 37 °C for 1 day, 3 days, 7 days, and 30 days. At predetermined time points (1, 24, 48 ...720 hours), 1 ml of the buffer medium was collected and substituted with fresh buffer. The concentration of BSA in buffer medium was determined by measuring the absorbance

Open Access Article. Published on 07 May 2024. Downloaded on 12/5/2025 8:51:53 PM.
This article is licensed under a Creative Commons Attribution-NonCommercial 3.0 Unported Licence.

at 280 nm using a UV-vis spectrometer (HITACHI, U-5100). Then, the concentration of adhered proteins on uncoated and P60-coated UCs was calculated and compared. The calculation formula used is as follows:

$$\text{Inhibition (\%)} = \frac{\text{BSA adhered on uncoated UCs} - \text{BSA adhered on coated UCs}}{\text{BSA adhered on uncotaed UCs}} \times 100$$

2.5. *In vitro* cell viability

In vitro cytocompatibility of uncoated and P60-coated UCs was evaluated by the MTT assay tested against NCTC clone 929 [L cell, L-929, derivative of strain L] (CCL-1™) mouse fibroblast cell line following a standard protocol described elsewhere.[40] Briefly, L-929 cells were regenerated, seeded to flask in complete DMEM medium supplemented with 10% (v:v) FBS, 1% (v:v) L-glutamine, and 1% (v:v) penicillin–streptomycin and cultured in a humidified 5% CO_2 environment. Prior to cell seeding, cells were dissociated with 0.25% trypsin–0.05% EDTA solution, centrifuged and resuspended in the complete medium. 100 000 L-929 cells were seeded onto each tissue culture plate surface (TCPS) of a 24 multi-well plate and incubated for 24 hours to obtain a monolayer culture. Afterwards the culture medium was removed and gently washed with DPBS to eliminate dead/unbound cells. Following this, uncoated or P60-coated UC substrates were treated with UV germicidal irradiation (λ = 254 nm) for an hour, transferred to the wells and incubated in the medium for 24 hours. TCPS and uncoated catheter substrates (UCs) were used as the negative control and control, respectively. At the end of 24 hours of incubation time, the media were aspirated, and dead or unbound cells were removed; wells were washed with DPBS gently. After further washing, FBS-free medium containing 0.5 mg ml^{-1} of MTT was added to each well. After 4 hours of incubation, media were gently aspirated and washed with DPBS. To assess the viability of the cells, formazan crystals were dissolved in DMSO and optical densities were spectrophotometrically measured using a microplate reader (Thermo Scientific, Multiskan GO Microplate Photometer) at 540 nm.

3. Results and discussion

3.1. Chemical structure analysis of PEG-like films

FTIR analysis was conducted to determine the chemical composition of the PEG-like film surfaces created by plasma processing at 5 W for different plasma exposure times (15, 30 and 60 min), respectively (Fig. 1a). For the PEG precursor, one of the characteristic bands is –OH stretching vibration that appeared in the region of 3630–3040 cm^{-1}. Other pronounced bands such as symmetric and asymmetric –CH_2 peaks were observed at 2930 cm^{-1} and 2864 cm^{-1}, respectively. In addition, –CH_2 bending vibrations were observed at 1462 cm^{-1} and between 970 cm^{-1} and 790 cm^{-1}. The –C–C– stretching vibrations for PEG were also detected between 1400 cm^{-1} and 1200 cm^{-1}. The double bands for –C–O–C– stretching vibrations found at 1115 cm^{-1} and 1060 cm^{-1} were the main characteristic peaks of PEG. The spectra for PEG precursor were compared with spectra of PEG-like films as shown in Fig. 1a. Characteristic PEG peaks (–CH_2 peaks and –OH peak and –C–O–C– peaks) were also seen in spectra of all PEG-like films. However, an additional peak was detected at 1725 cm^{-1}, which was attributed to the –C═O stretching vibrations. These carbonyl groups can be formed by oxidative degradation when exposed to air (oxygen) after the process. Several research studies confirmed these results as well.[41,42] As conclusions, FTIR results confirmed that PEG-like films were successfully deposited on the substrates, and they possessed chemical similarity to PEG precursor.[41]

The effect of plasma exposure time on the chemical structure of PEG-like films was also investigated. Herein, plasma polymerization proceeded at 5 W for 15 min, 30 min and 60 min. It was observed that as the plasma exposure time increased, the intensity of –OH decreased and –C–O–C increased. Detailed information about percentage areas of the corresponding chemical bonds can be found in the ESI† (S2).

Furthermore, the stability of the films was assessed through FTIR analysis. The solubility of PEG molecules is known to be very high, especially those with a low molecular weight.[43] In this study, soluble characteristic has been manipulated with crosslinks that originated as a result of plasma polymerization technique. P60 thin films underwent multiple rinses with DI water and organic solvents such as methanol and ethanol. The FTIR spectra of PEG-like films before and after rinsing are depicted in S3 (ESI†). Remarkably, no discernible differences were observed between the FTIR spectra of the rinsed thin films and the PEG-like film. This phenomenon can be attributed to the presence of crosslinks between the PEG chains formed during polymerization as it was mentioned in the literature.[44] Moreover, there was no evidence of delamination observed during rinsing, indicating strong chemical adhesion of the films to the substrates. This outcome aligns with expectations, as the substrates were treated at base pressure with RF plasma for 1 min prior to plasma polymerization, facilitating enhanced adhesion between the films and substrates.

3.2. XPS analysis of PEG-like films

XPS analysis was performed to determine the compositional changes of PEG-like films with variations in the plasma exposure time. High-resolution C (1s) spectra of the P15, P30 and P60 films are presented in Fig. 1b–d. C (1s) photoelectron region was deconvoluted into four separate binding energy peaks corresponding to –C–C bonds (284.8 eV), –C–O–H (286.4 eV), –C–O–C (286.6 eV), and –C═O (288.9 eV), respectively. XPS results of PEG-like films are also tabulated in Table S2 in S4 (ESI†). It is known that the majority of PEG polymers consists of –C–O–C bond related to the PEO character, based on the peak area of the –C–O–C bond.[32,45] XPS results demonstrate significant variations in the chemical structure of PEG-like films with respect to the plasma exposure time. After plasma

 This journal is © The Royal Society of Chemistry 2024

Open Access Article. Published on 07 May 2024. Downloaded on 12/5/2025 8:51:53 PM.
This article is licensed under a Creative Commons Attribution-NonCommercial 3.0 Unported Licence.

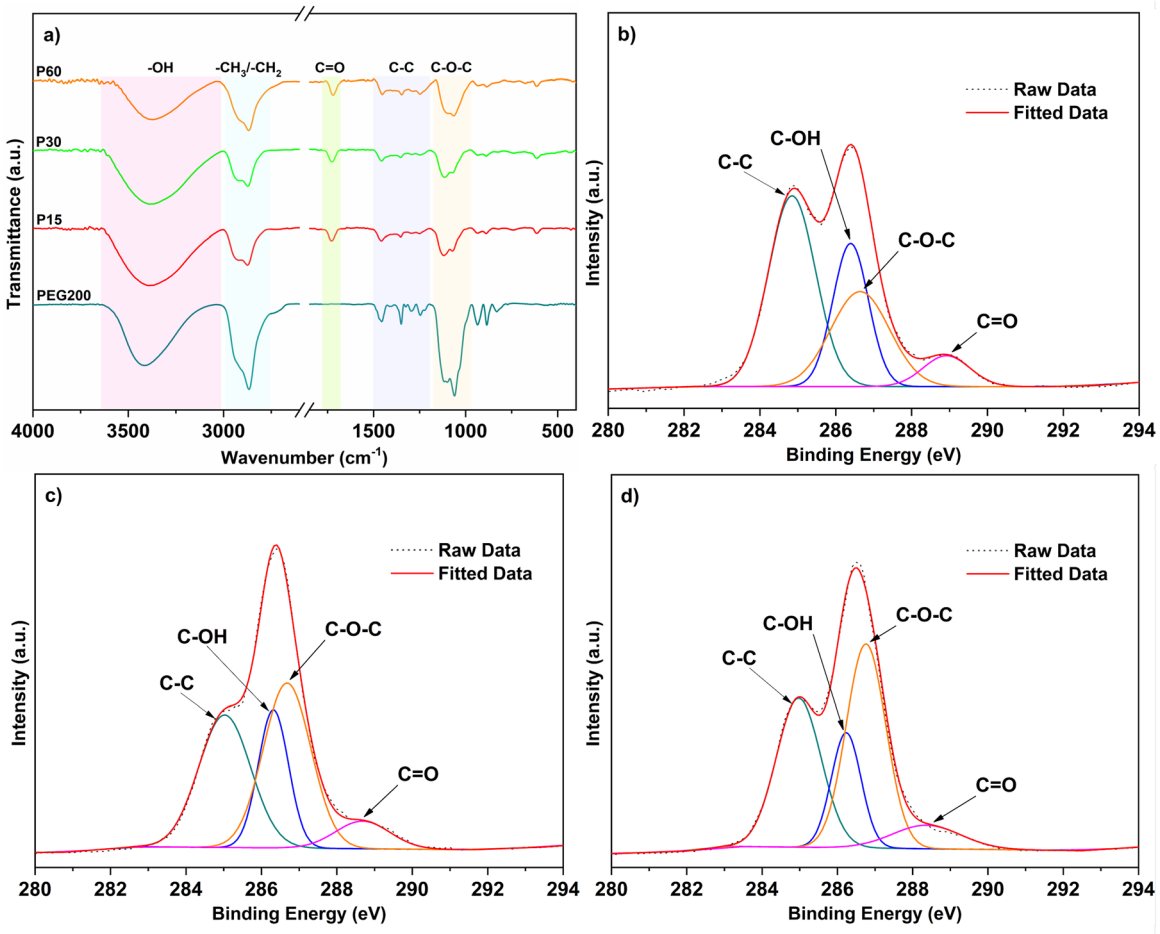

Fig. 1 (a) FTIR spectra of PEG-like thin films on silicone wafers. (b)–(d) Deconvoluted high resolution C 1s XPS spectra of P15, P30 and P60 films on glass slide, respectively. C–C bond (dark green); C–O–H bond (blue); C–O–C bond (orange) and C═O bond (magenta).

polymerization for 15 min, P15 consisted of 42.6% C–C bond, 26.4% –C–O–C bond, 24.1% C–OH and 6.9% –C═O bonds. As plasma polymerization continued for 60 min, the amount of –C–O–C bonds in films increased by 53.8%, whereas –C–C bond decreased by 20.8%. In other words, the C–O–C/C–C ratio increased with increasing the plasma exposure time. This implies a greater retention of the ethylene oxide structure in the PEG-like thin films produced *via* long plasma polymerization. In addition, –C–OH was reduced from 24.1% to 20.5% and then to 17.3% with increasing exposure time from 15 to 30 min and to 60 min, respectively.

3.3. Wettability of PEG-like films

The level of hydrophilicity and oleophilicity of PEG-like thin films were evaluated by measuring the contact angle of deionized water (WCA) and diiodomethane (DCA). Substrate (glass slide) was partially wettable with deionized water and diiodomethane (WCA and DCA $< 45 \pm 3^{\circ}$). As shown in Fig. 2, when PEG-like films were deposited on wafers, deionized water and oil spreadability on the surface was significantly changed. Even after plasma polymerization for 15 min, WCA and DCA increased up to the level of 86.7° and 69.0°, respectively.

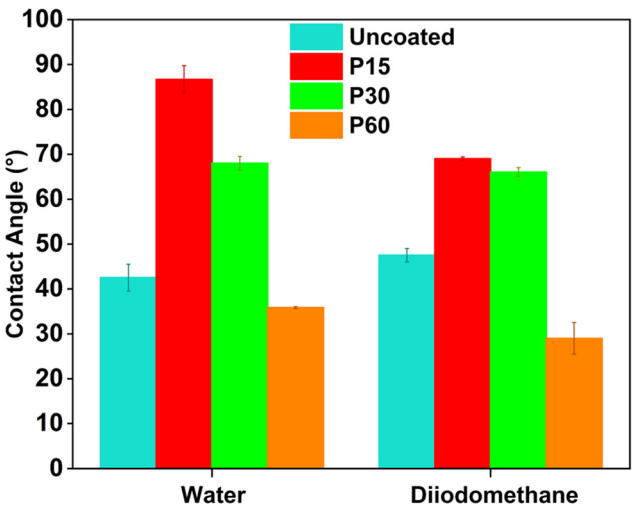

Fig. 2 The contact angle of deionized water (polar) and diiodomethane (dispersive) on uncoated and PEG-like coated glass slides.

However, when more PEG chains were deposited on the surface with increasing plasma exposure time (up to an hour), WCA

Open Access Article. Published on 07 May 2024. Downloaded on 12/5/2025 8:51:53 PM. This article is licensed under a Creative Commons Attribution-NonCommercial 3.0 Unported Licence.

Table 1 Surface wettability analysis of samples synthesized with PE-CVD

Sample	Wettability (°)	Dispersive component (mJ cm^{-2})	Polar component (mJ cm^{-2})	Total surface free energy (mJ cm^{-2})
Uncoated	42.74 ± 3.29	35.70	24.38	60.09
P15	86.66 ± 3.82	23.47	4.98	28.45
P30	67.79 ± 1.46	25.83	13.72	39.55
P60	39.78 ± 6.22	44.24	21.78	66.02

and DCA decreased to 39.8° and 30°, respectively. This is expected to be due to its enrichment with more –C–O–C groups produced during plasma polymerization. It is worth to say that P60 films possess similar hydrophilic and oleophilic features to the PEG films synthesized by dip coating, where similar contact angle measurements ($WCA_{PEG} \approx 37.3°$ and $DCA_{PEG} \approx 29°$) were reported.[46]

Surface energy (σ) of PEG-like coatings influences surface properties of coatings. Thus, their surface energies were estimated using their WCA and DCA results according to the Owens–Wendt method (S5, ESI†). The surface energy of PEG-like coatings is shown in Table 1. Surface energy of coatings depended on the plasma exposure time. Among the thin films, P60 exhibited the highest surface energy, 66.02 mJ cm^{-2}, whereas P30 and P15 exhibited 39.55 mJ cm^{-2} and 28.45 mJ cm^{-2}, respectively. Surface energy value for reference glass slide was 60.09 mJ cm^{-2}; therefore, the comparisons between coated and reference surfaces showed that 60 min thin film synthesis enhances surface free energy likewise hydrophilicity of sample surfaces. XPS results revealed that as the plasma exposure time increased, the amount of non-polar –C–C bonds of the thin films decreased and the polar –C–O–C group increased, which affected the increase in surface energy behavior.

3.4. Antimicrobial/antifouling properties of PEG-like films

In vitro antimicrobial/antifouling tests were conducted with *P. mirabilis* and *E. coli* bacterial strains, as these are the most commonly isolated bacteria from urinary catheter biofilms.[33] Thus, antifouling coatings on catheters are required to repel from the sample surface and/or kill them by contact. Some studies have reported antibacterial properties of PEG coatings incubated for short periods (<8 days), as PEG chains are easily oxidised in the presence of O_2, forming ethers and aldehydes.[47,48] This reaction causes the degradation of PEG with a consequent reduction of PEG coatings' antifouling ability. Therefore, they have a limited utility in long-term applications.[49,50] Especially, for urinary catheter applications, coatings on urinary catheters should be durable for more than 7 days.[51] Hence, we synthesized PEG-like thin film on catheters *via* the PE-CVD technique to investigate the long-term effect as well. PEG chains become crosslinked during plasma coating, leading to the formation of highly durable PEG-like films. And, since the P60 thin film exhibits the lowest contact angle with higher C–O–C groups, microbiological studies were carried on only P60 samples. The concentration of *P. mirabilis* and *E. coli* on P60-coated and uncoated catheters was examined after incubation for 1 day, 3 days, 7 days, and 30 days. The quantitative analysis of each bacterial colony was performed using colony forming units (CFU) per milliliter (CFU ml^{-1}), shown in Fig. 3 and 4. To assess potential contamination and bacterial growth prior to assay analysis, bacterial multiplication was assessed using fresh and sterile TSA agar plates. Fig. 3a and b illustrate the number of *P. mirabilis* present on the uncoated and coated UCs after incubation for 1, 3, 7 and 30 days. It was found that *P. mirabilis* was extensively present in the environment of the uncoated UCs within the first 24 h of incubation. As expected, the number of colonies increased from 4.8×10^7 CFU ml^{-1} to 7.0×10^7 CFU ml^{-1}, and then 1.2×10^8 CFU ml^{-1} as incubation time increased from 24 hours to 3 days and 7 days, respectively. After a month (30 days) of incubation, the concentration of *P. mirabilis* on uncoated catheter surfaces reached up to 8.5×10^{10} CFU ml^{-1}. On the other hand, a significant decrease in the adhesion of *P. mirabilis* on P60-coated UCs was observed as compared with uncoated ones. Even though the antifouling mechanism process is complicated, the bacterial repellency (%) for P60-coated UCs increased with increasing incubation time (Fig. 3a). After 1 day of incubation, P60 coatings repelled 44.83% of *P. mirabilis* bacteria, whereas 73.00% and 93.90% of bacteria were repelled after 7 days and 30 days of incubation, respectively. Furthermore, unbound *P. mirabilis colonies* on catheters were also observed, shown in Fig. 3b. This indicates that the number of unbound cells on P60-coated UCs increased with increasing incubation time. In addition, there is no significant unbound cell concentration differences between uncoated UCs and P60-coated UCs.

Fig. 4a shows that, for the uncoated UC substrates, the concentration of *E. coli* live bacteria was found to be approximately 4.8×10^6 at the end of the first 24 hours of incubation and continued to increase exponentially to 1.5×10^{11} CFU ml^{-1} at the end of 30 days of incubation. Meanwhile, P60-coated UC surfaces limited the adherence of *E. coli* live bacteria concentration down to 3.1×10^6 CFU ml^{-1} (24-hour incubation) and 4×10^9 CFU ml^{-1} (30-day incubation), corresponding to 34.5% and 97.3% of inhibition ratios respectively. On the other hand, Fig. 4b shows the concentration of live *E. coli* bacteria that could not adhere to the surfaces and maintained their viability during the incubation period. Details about ONE-WAY ANOVA test is given in the ESI† (S6).

For both *P. mirabilis* overgrowth and *E. coli* strain overgrowth, proliferation can be related to the humidity of the environment (~15%) and to the TSB medium used, which provides a suitable environment for the bacterial species to adhere and grow on the substrate surfaces. SEM images were taken to confirm the observed trend in live bacterial concentration

 This journal is © The Royal Society of Chemistry 2024

Open Access Article. Published on 07 May 2024. Downloaded on 12/5/2025 8:51:53 PM.
This article is licensed under a Creative Commons Attribution-NonCommercial 3.0 Unported Licence.

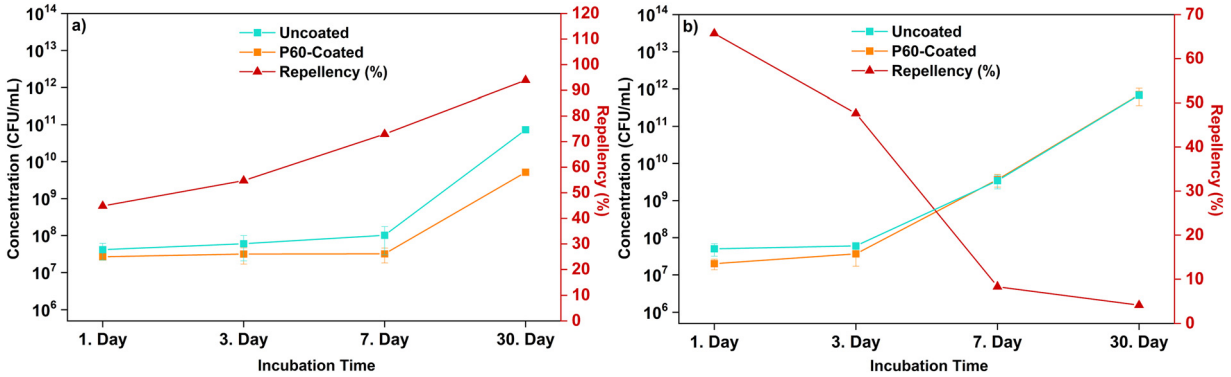

Fig. 3 Bacteria colonization of *P. mirabilis*. (a) Bacterial colonies adhered to the P60-coated and uncoated UC surfaces, and red shows the bacteria repellency (%) from the P60-coated UC. (b) Bacterial colonies that were not adhered on the P60-coated and uncoated UC surfaces when immersed in a wash buffer (PBS). Bacterial strains were cultivated on TSA plates, and each bacterial strain was incubated with the substrate of interest for 24, 72, 168 h and 30 days at 37 °C (n = 6).

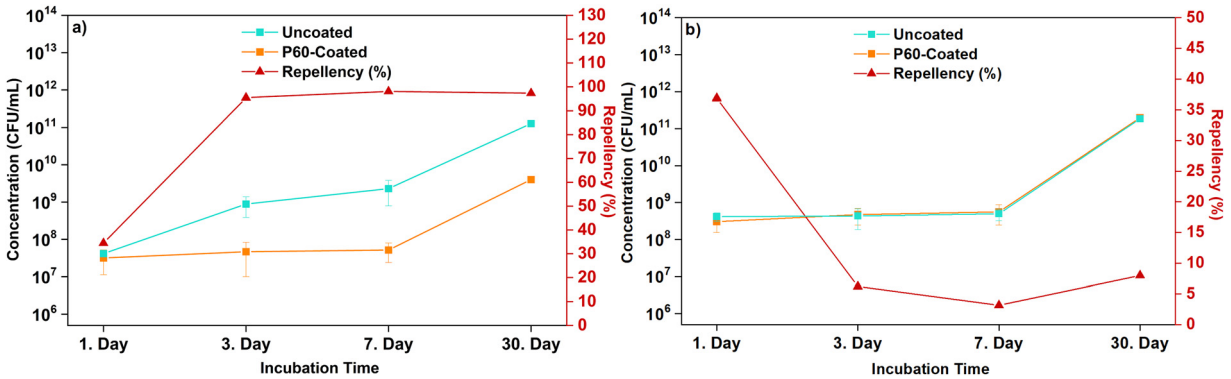

Fig. 4 Bacteria colonization of *E. coli*. (a) Bacterial colonies adhered to the P60-coated and uncoated UC surfaces, and red shows the bacteria repellency (%) from the P60-coated UC. (b) Bacterial colonies that were not adhered on the P60-coated and uncoated UC surfaces when immersed in a wash buffer (PBS). Bacteria strains were cultivated on TSA plates, and each bacterial strain was incubated with the substrate of interest for 24, 72, 168 h and 30 days at 37 °C (n = 6).

(CFU/ml) for UCs and P60-coated substrates for both bacterial strains for different incubation times (24h, 72h, 168h and 30 days). Fig. 5 and 6 clearly show that uncoated UC surfaces are considerably much more conducive to bacterial adhesion for both strains, whereas P60-coated UCs restricted bacterial adhesion noticeably. It can be also said that P60-coated UC surfaces also prevent the colony formation of bacterial strains and also limit the growth rate of bacterial strains which were adhered to the surfaces. This feature of the PEG coating can be explained by the surface repellent property of PEG towards the studied bacterial strains, which also limits the metabolic activity of the mentioned bacterial strains, that ended up with a slower growth rate and less colonization ability compared to the uncoated UC ones.[52,53]

3.5. Protein adhesion studies

Specifically, silicone-based catheters were coated with PEG-like films *via* PE-CVD. In this part, only P60 films were deposited on catheters since they possess high –C–O–C bonds, which refers to ''PEO character'' affecting antifouling feature. In addition, P60 films are highly hydrophilic as compared to the other thin films (P15 and P30). To demonstrate the PEG-coated UCs as protein fouling resistant materials, bovine serum albumin (BSA) protein was used. BSA is negatively charged and rich in deprotonated carboxylic acid groups.[54]

The presence of aforementioned groups was also found in blood plasma and involved in supply nutrients. Herein, a series of BSA adsorption experiments were carried out at pH 7.4 and at 37 °C. Uncoated UCs and P60-coated UCs were kept in BSA solution (1 mg ml^{-1}, dissolved in PBS buffer). The level BSA adsorption on catheters was calculated at different times. The results are shown in Fig. 7. This demonstrates that after 1 h of incubation, uncoated UCs and P60-coated UCs had BSA adsorption levels of 2.89% and 1.55%, respectively. Over a 48 h incubation period, unmodified UCs adsorbed 29.51% of the BSA protein. In addition, the P60 film demonstrated a reduction in the amount of protein adhered to the catheters by 22.58% compared to the uncoated ones. This indicates the efficacy of the P60 film in reducing protein adsorption on catheter surfaces. Up to 30 days of incubation, for uncoated UCs, the BSA adsorption level significantly increased (41.70%).

Open Access Article. Published on 07 May 2024. Downloaded on 12/5/2025 8:51:53 PM.
This article is licensed under a Creative Commons Attribution-NonCommercial 3.0 Unported Licence.

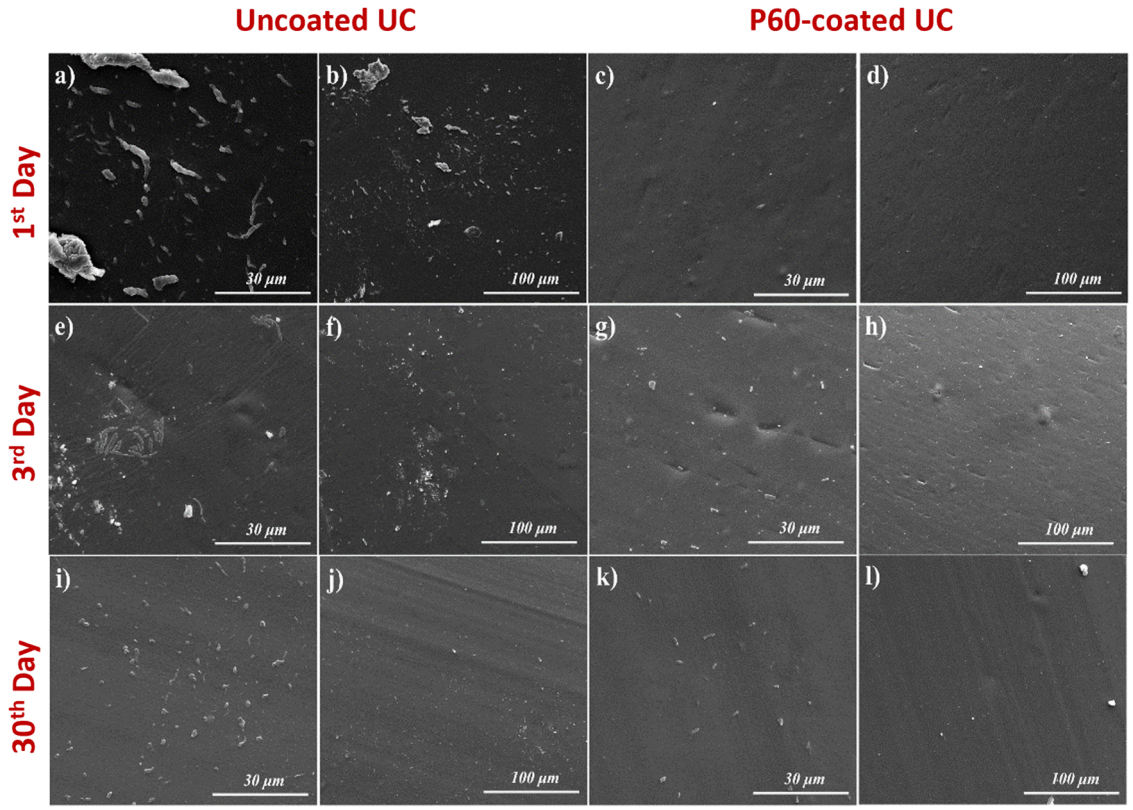

Fig. 5 SEM images of UCs and P60-coated UCs of *P. mirabilis*. a–b, e–f, i–j related to uncoated and c–d, g–h, k–l related to P60-coated UCs. The magnification of the first and the third column is 2500× and the magnification for the second and the fourth column is 500×.

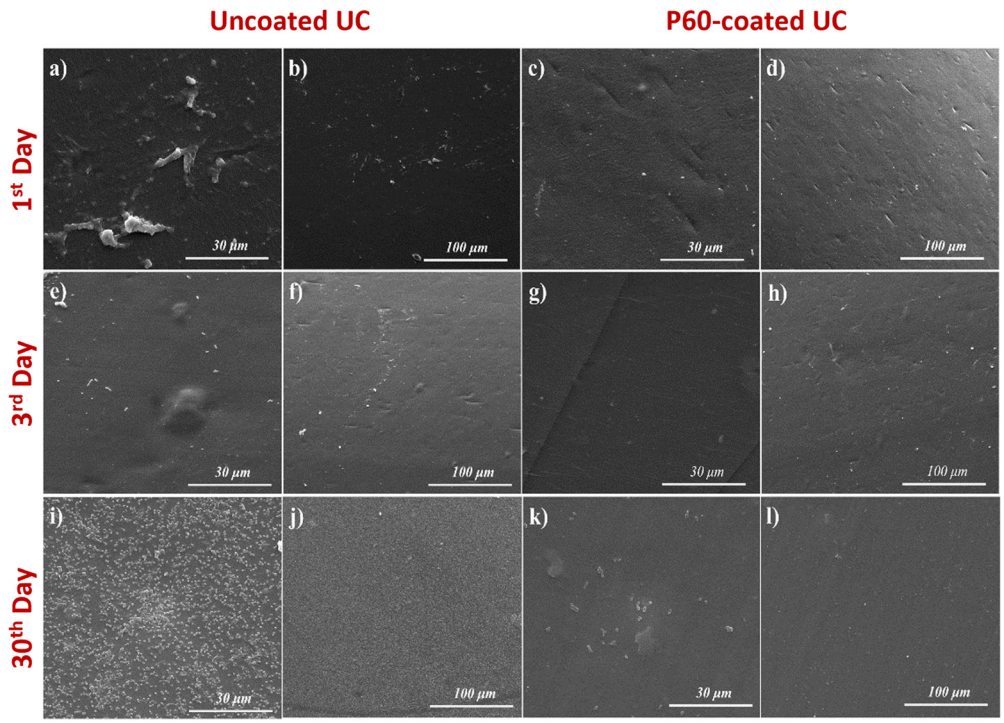

Fig. 6 SEM images of UCs and P60-coated UCs of *E. coli*. a–b, e–f, i–j related to uncoated and c–d, g–h, k–l related to P60-coated UCs. The magnification of the first and the third column is 2500× and the magnification for the second and the fourth column is 500×.

 This journal is © The Royal Society of Chemistry 2024

Open Access Article. Published on 07 May 2024. Downloaded on 12/5/2025 8:51:53 PM.
This article is licensed under a Creative Commons Attribution-NonCommercial 3.0 Unported Licence.

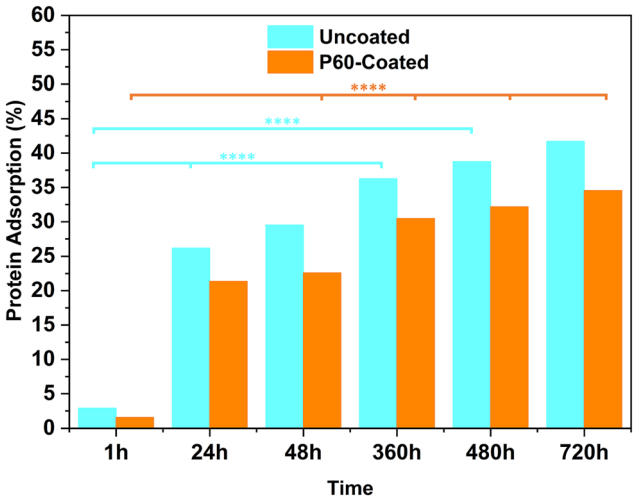

Fig. 7 BSA protein adsorption on uncoated and P60-coated UCs (n = 6) (***p < 0.005,****p < 0.001). Remaining p values did not express a significant difference.

However, for P60-coated UCs, it is slightly increased in 30 days and reached 34.52% adsorption level. It is important to note that although there was an increase in the PEG-modified samples at the end of 30 days, the difference with the uncoated was around 20%. As the samples were treated in a dynamic environment, this situation also has a negative effect on surface stability. As PBS is a charged buffer medium in terms of ions (*i.e.* Na, K *etc.*), the interaction between PEG-like coatings and buffer media is inevitable.[55] Nevertheless, it can be concluded that P60-coated catheters can be safely used in clinical applications compared to current catheters.

3.6. *In vitro* cell viability

According to the ISO 10993-5 standard, biomaterials should not decrease cell viability under 70% to fulfill the non-toxicity features.[56] The biocompatible property of silicone makes it a popular polymeric material in biomedical applications, including urinary catheter bulk structures.[57]

As the UCs will be in contact with a physiological environment, they have to fulfill several quality standards, including biocompatibility and safety, in order to be used by patients. Therefore, to evaluate the biocompatibility of the PEG coated UCs, their cytotoxicity against L-929 cell line was tested. *In vitro* cytotoxicity results shown in Fig. 8 indicate that compared to the TCPS control (100.00 ± 13.93%), both UC and UC-PEG enhanced cellular viability, yielding 127.06 ± 14.91% (****p < 0.001) and 108.95 ± 10.82% (****p < 0.001), respectively. Even though reference UCs have a higher value of fibroblast viability compared to UC-PEG ones, there is still no cytotoxic effect of the modified UC substrates on the mentioned cell line.

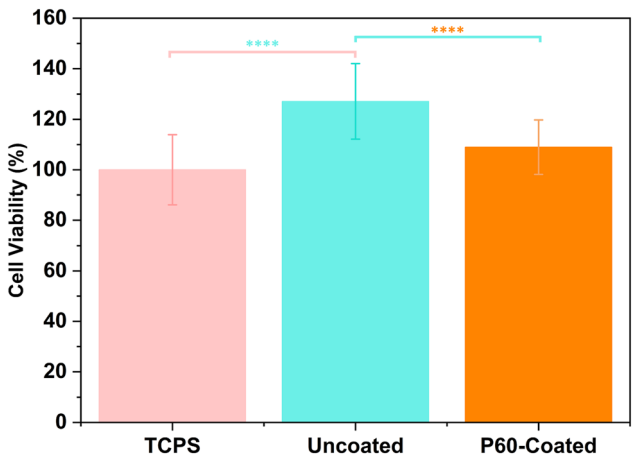

Fig. 8 Cell viability of uncoated and P60-coated urinary catheters (****p < 0.001).

4. Conclusions

PEG-like thin films were deposited using the PE-CVD technique on different substrates including urinary catheters, using a single plasma precursor. To the best of our knowledge, the low molecular weight PEG200 precursor was employed for the first time to synthesize thin films with this technique and investigate the long-term antifouling potency against uropathogenic bacteria for up to 30 days along with the possible toxicity with mouse fibroblast cell line and protein adsorption analysis. FTIR and XPS results revealed that the molecular structure of PEG200 was retained at 20 mTorr vapor pressure and at a low plasma power. Moreover, longer plasma exposure time improved the PEO character of the coating and increased the wettability of the surfaces. In pursuance of analysis result, it was concluded that PEG-like coatings made in 60 minutes offer the most effective antifouling barrier for bacterial encounter on surfaces with the bacterial repellency rate of 93.9% for *P. mirabilis* and 97.3% for *E. coli* at the end of the 30-day period. Besides, it was determined that PEG like thin film coated catheters do not possess any toxicity instead they promote cell viability and proliferation with quite lower protein adsorption compared to uncoated catheters.

Conflicts of interest

There are no conflicts to declare.

Acknowledgements

This study was supported by Scientific and Technological Research Council of Turkey (TUBITAK) under the Grant Number 221S775. The authors thank to TUBITAK for their supports.

References

1 K. G. Neoh, M. Li, E. T. Kang, E. Chiong and P. A. Tambyah, *J. Mater. Chem. B*, 2017, **5**, 2045–2067.

Open Access Article. Published on 07 May 2024. Downloaded on 12/5/2025 8:51:53 PM. This article is licensed under a Creative Commons Attribution-NonCommercial 3.0 Unported Licence.

2 C. A. Umscheid, M. D. Mitchell, J. A. Doshi, R. Agarwal, K. Williams and P. J. Brennan, *Infect. Control Hosp. Epidemiol.*, 2011, **32**, 101–114.
3 K. Clarke, C. L. Hall, Z. Wiley, S. Chernetsky Tejedor, J. S. Kim, L. Reif, L. Witt and J. T. Jacob, *J. Hosp. Med.*, 2020, **15**, 552–556.
4 C. E. Chenoweth, C. V. Gould and S. Saint, *Infect. Dis. Clin. North Am.*, 2014, **28**, 105–119.
5 B. Foxman, *Nat. Rev. Urol.*, 2010, **7**, 653–660.
6 S. A. Wilks, V. V. Koerfer, J. A. Prieto, M. Fader and C. W. Keevil, *mBio*, 2021, **12**(2), 10–1128.
7 P. Singha, J. Locklin and H. Handa, *Acta Biomater.*, 2017, **50**, 20–40.
8 S. Anjum, S. Singh, L. Benedicte, P. Roger, M. Panigrahi and B. Gupta, *Glob. Challenges*, 2018, **2**, 1700068.
9 C. M. C. Faustino, S. M. C. Lemos, N. Monge and I. A. C. Ribeiro, *Adv. Colloid Interface Sci.*, 2020, **284**, 102230.
10 X. Li, B. Wu, H. Chen, K. Nan, Y. Jin, L. Sun and B. Wang, *J. Mater. Chem. B*, 2018, **6**, 4274–4292.
11 C. Diaz Blanco, A. Ortner, R. Dimitrov, A. Navarro, E. Mendoza and T. Tzanov, *ACS Appl. Mater. Interfaces*, 2014, **6**, 11385–11393.
12 P. Kingshott, J. Wei, D. Bagge-Ravn, N. Gadegaard and L. Gram, *Langmuir*, 2003, **19**, 6912–6921.
13 N. Mahmood Aljamali and I. Obaid Alfatlawi, *Int. J. Thermodyn. Chem. Kinetics*, 2021, **7**, 1–8.
14 A. G. Ulyashin, A. Hadjadj and M. A. Butt, *Coatings*, 2022, **12**, 1115.
15 B. R. Coad, P. Favia, K. Vasilev and H. J. Griesser, *Plasma Process. Polym.*, 2022, **19**, 2200121.
16 K. L. Choy, *Chemical Vapour Deposition (CVD): Advances, Technology and Applications*, CRC Press, 1st edn, 2019.
17 A. Asatekin, M. C. Barr, S. H. Baxamusa, K. K. S. Lau, W. Tenhaeff, J. Xu and K. K. Gleason, *Mater. Today*, 2010, **13**, 26–33.
18 in *Chemical vapor deposition*, ed. J. H. Park, and T. S. Sudarshan, ASM international, Ohio, Cleveland, 2001, vol. 2.
19 J. O. Carlsson and P. M. Martin, *Chemical vapor deposition*, William Andrew Publishing, 2010.
20 K.-H. Dahmen, *Encycl. Phys. Sci. Technol.*, 2003, 787–808.
21 E. Sanchez Armengol, A. Unterweger and F. Laffleur, *Drug Dev. Ind. Pharm.*, 2022, **48**, 129–139.
22 S. Sun, Y. Cui, B. Yuan, M. Dou, G. Wang, H. Xu, J. Wang, W. Yin, D. Wu and C. Peng, *Front. Bioeng. Biotechnol.*, 2023, **11**, 1117647.
23 K. Knop, R. Hoogenboom, D. Fischer and U. S. Schubert, *Angew. Chem., Int. Ed.*, 2010, **49**, 6288–6308.
24 G. Gelardi, S. Mantellato, D. Marchon, M. Palacios, A. B. Eberhardt and R. J. Flatt, *Sci. Technol. Concr. Admixtures*, 2016, 149–218.
25 J. Wu, C. Zhao, W. Lin, R. Hu, Q. Wang, H. Chen, L. Li, S. Chen and J. Zheng, *J. Mater. Chem. B*, 2014, **2**, 2983–2992.
26 J. Kim, H. K. Shon, S. Joh, D. Jung, H. K. Na and T. G. Lee, *Surf. Coatings Technol.*, 2020, **403**, 126384.
27 A. Choukourov, I. Gordeev, D. Arzhakov, A. Artemenko, J. Kousal, O. Kylián, D. Slavínská and H. Biederman, *Plasma Process. Polym.*, 2012, **9**, 48–58.
28 E. Sardella, F. Palumbo, G. Camporeale and P. Favia, *Mater.*, 2016, **9**, 515.
29 G. P. Löpez, B. D. Ratner, C. D. Tidwell, C. L. Haycox, R. J. Rapoza and T. A. Horbett, *J. Biomed. Mater. Res.*, 1992, **26**, 415–439.
30 T. Dufour, *Polymers*, 2023, **15**(17), 3607.
31 B. Nisol, C. Poleunis, P. Bertrand and F. Reniers, *Plasma Process. Polym.*, 2010, **7**, 715–725.
32 C. Choi, I. Hwang, Y. L. Cho, S. Y. Han, D. H. Jo, D. Jung, D. W. Moon, E. J. Kim, C. S. Jeon, J. H. Kim, T. D. Chung and T. G. Lee, *ACS Appl. Mater. Interfaces*, 2013, **5**, 697–702.
33 J. Miao, X. Wu, Y. Fang, M. Zeng, Z. Huang, M. Ouyang and R. Wang, *J. Mater. Chem. B*, 2023, **11**, 3373–3386.
34 D. S. Lee, S. J. Lee and H. S. Choe, *Biomed Res. Int.*, 2018, **2018**, DOI: **10.1155/2018/7656752**.
35 B. Köves, A. Magyar and P. Tenke, *GMS Infect. Dis.*, 2017, **5**, 1–5.
36 P. Behzadi, *Microbiol. Urin. Tract Infect. – Microb. Agents Predisposing Factors, S. S. Long, Princ. Pract. Pediatr. Infect. Dis.*, 4th edn, 2012, pp. 1–1712.
37 A. N. Norsworthy and M. M. Pearson, *Trends Microbiol.*, 2017, **25**, 304.
38 T. Tailly, R. A. MacPhee, P. Cadieux, J. P. Burton, J. Dalsin, C. Wattages, J. Koepsel and H. Razvi, *J. Endourol.*, 2021, **35**, 116–121.
39 H. F. Özgüzar, E. Evren, A. E. Meydan, G. Kabay, J. S. Göçmen, F. Buyukserin and O. Erogul, *Adv. Mater. Interfaces*, 2023, **10**, 2202009.
40 H. F. Özgüzar, A. E. Meydan, J. S. Göçmen and M. Mutlu, *MRS Commun.*, 2021, **11**, 523–531.
41 S. Gaiser, U. Schütz, P. Rupper and D. Hegemann, *Mol.*, 2020, **25**, 6024.
42 A. Choukouro, I. Gordeev, O. Polonskyi, A. Artemenko, L. Hanyková, I. Krakovský, O. Kylián, D. Slavínská and H. Biederman, *Plasma Process. Polym.*, 2010, **7**, 445–458.
43 B. Ensing, A. Tiwari, M. Tros, J. Hunger, S. R. Domingos, C. Pérez, G. Smits, M. Bonn, D. Bonn and S. Woutersen, *Nat. Commun.*, 2019, **10**, 1–8; Y. Wu, S. Joseph and N. R. Aluru, *J. Phys. Chem. B*, 2009, **113**, 3512–3520.
44 Y. Wu, S. Joseph and N. R. Aluru, *J. Phys. Chem. B*, 2009, **113**, 3512–3520.
45 I. Gordeev, A. Choukourov, O. Polonskyi, D. Slavinska and H. Biederman, *WDS'09 Proceedings of Contributed Papers, Part III*, 2009, 182–188.
46 B. Ö. Yılmaz, Master's thesis, Istanbul Medipol University, 2021.
47 F. Kawai, *Appl. Microbiol. Biotechnol.*, 2002, **58**, 30–38.
48 G. Cheng, Z. Zhang, S. Chen, J. D. Bryers and S. Jiang, *Biomaterials*, 2007, **28**, 4192–4199.
49 Z. Yang, Z. Yang, X. Lv, G. Jiang, X. Zhang, X. Li, X. Li, R. Yuan and Y. Zhuo, *Chem. Eng. J.*, 2023, **454**, 140490.
50 I. Banerjee, R. C. Pangule, R. S. Kane, I. Banerjee, R. C. R. S. Pangule and H. P. Kane, *Adv. Mater.*, 2011, **23**, 690–718.
51 L. Mi and S. Jiang, *Angew. Chem., Int. Ed.*, 2014, **53**, 1746–1754.

 This journal is © The Royal Society of Chemistry 2024

Open Access Article. Published on 07 May 2024. Downloaded on 12/5/2025 8:51:53 PM.
This article is licensed under a Creative Commons Attribution-NonCommercial 3.0 Unported Licence.

52 C. Ungureanu, C. Pirvu, M. Mindroiu and I. Demetrescu, *Prog. Org. Coat.*, 2012, **75**, 349–355.
53 S. Chen, L. Li, C. Zhao and J. Zheng, *Polymer*, 2010, **51**, 5283–5293.
54 B. E. Givens, N. D. Diklich, J. Fiegel and V. H. Grassian, *Biointerphases*, 2017, **12**, 2, DOI: **10.1116/1.4982598**.
55 M. Son, Y. S. Lee, M. J. Lee, Y. K. Park, H. R. Bae, S. Y. Lee, M. G. Shin and S. Yang, *PLoS One*, 2021, **16**(12), DOI: **10.1371/journal.pone.0262106**.
56 10993-5, I. S. O. I. 2009 Biological evaluation of medical devices—part 5: tests for in vitro cytotoxicity, **https://www.iso.org/standard/36406.html**, (Accessed November 15, 2023).
57 M. J. Whitford, *Biomaterials*, 1984, **5**, 298–300.